Tellus (1999), 51A, 603–611
Printed in UK. All rights reserved

TELLUS
ISSN 0280–6495

The slope of isentropes constituting a frontal zone

By AARNOUT VAN DELDEN, *Institute for Marine and Atmospheric Sciences, Utrecht University, Princetonplein 5, 3584 CC Utrecht, The Netherlands*

(Manuscript received 29 September 1998; in final form 31 May 1999)

ABSTRACT

This paper investigates the use of the slope of isentropes as an objective indicator of the presence of frontal zones in the atmosphere. It derives an equation for the change in time relative to the front of the slope of isentropes and applies this equation to a specific case. It discusses the advantages and disadvantages of this approach and compares it with the traditional approach based on the horizontal temperature gradient. It appears that the use of the slope of isentropes to identify fronts brings out some features of frontal systems more clearly than the traditional definition, especially cold fronts which lean forward toward the warm air. Three new frontogenetic terms appear in the equation governing the time rate of change of frontal intensity. In the particular case studied here, these frontogenetic terms cannot be neglected, although they play only a secondary rôle

1. Introduction

Since the appearance of the textbook on synoptic meteorology by Petterssen (1940, 1956) and the paper on frontogenesis by Miller (1948), the intensity of a front in the atmosphere is usually defined as the absolute value of the horizontal gradient of a scalar such as the potential temperature. Miller (1948) identified the mechanisms contributing to changes in frontal intensity by deriving an equation for the rate of change of frontal intensity according to his definition. This definition is also used in quasi-geostrophic theory (Holton, 1992). On the other hand, Renard and Clarke (1965) have identified the so-called "thermal front parameter", being the horizontal gradient of the magnitude of the gradient of the potential temperature, resolved into the direction of the gradient, as an indicator of the frontal location and intensity. This indicator has been the subject of several papers (Huber-Pock and Kress, 1989; Steinacker, 1992 and Hewson, 1998), but, to the authors knowledge, no attempt has been made to derive an equation for the change in time of the thermal front parameter. Probably this is due to the fact that the thermal front parameter was meant principally as a locator of fronts. Moreover, the mathematical complexity of the thermal front parameter makes it difficult to derive an equation for its time rate of change. Nevertheless, any definition of frontal intensity should include a definition of the time rate of change of frontal intensity, so that it can not only be used to locate fronts but also to identify frontal intensification or weakening as well as the physical effects leading to frontal intensification or weakening.

In this paper, another possible definition will be discussed. This definition relates the intensity and position of a front to the slope of isentropes with a vector, $\boldsymbol{I}_F$, defined as

$$\boldsymbol{I}_F = I_{Fx}\hat{\boldsymbol{i}} + \boldsymbol{I}_{Fy}\hat{\boldsymbol{j}} \equiv \left(\frac{\partial z}{\partial x}\right)_\theta \hat{\boldsymbol{i}} + \left(\frac{\partial z}{\partial y}\right)_\theta \hat{\boldsymbol{j}}$$

$$= -\left(\frac{\partial \theta}{\partial x}\left[\frac{\partial \theta}{\partial z}\right]^{-1}\hat{\boldsymbol{i}} + \frac{\partial \theta}{\partial y}\left[\frac{\partial \theta}{\partial z}\right]^{-1}\hat{\boldsymbol{j}}\right). \qquad (1)$$

E-mail: a.j.vandelden@phys.uu.nl.

In this equation, θ is the potential temperature, x, y and z are the zonal, meridional and vertical coordinates, respectively, I_{Fx} and I_{Fy} are the x- and y-components of the frontal intensity vector, respectively, and $\hat{i}$ and $\hat{j}$ are the unit vectors in the x- and y-directions, respectively. Mathematically, definition (1) differs from the definition due to Miller (1948) only by the factor $-(\partial\theta/\partial z)^{-1}$.

The definition according to (1), however, has several interesting and advantageous properties. First, frontal intensity is related to the orientation in space of a material surface, i.e., a surface of constant potential temperature. This implies that frontal intensification is related to the deformation and rotation of a material surface, which is physically easy to interpret and/or visualize. Second, sloping stable temperature-inversion layers are not considered a front as strongly as in the Miller–Petterssen definition. This is illustrated in the idealized example shown in Fig. 1. In fact, according to the above definition, an increase in the vertical (hydrostatic) stability, leaving the horizontal temperature gradient constant, leads to a weakening of the front (lower value of $|\boldsymbol{I}_F|$). Third, the stability of a front (i.e., the linear stability of thermal wind balance) is in fact governed by the slope of the isentropes and not exclusively by the absolute value of the gradient of the potential temperature. This is seen most clearly in the criterion for symmetric baroclinic instability, which states that the slopes of isentropes must exceed the slopes of linear momentum surfaces for instability (Holton, 1992, p. 281). But, it can also be seen in the three-dimensional problem by noting that the parameter governing baroclinic instability in, e.g., Holton's (1992) 2-layer model is proportional to the thermal wind (which, for an atmosphere in thermal wind balance, is proportional to the horizontal temperature gradient) divided by the static stability (see Fig. 8.3 of Holton (1992)). Therefore, $|\boldsymbol{I}_F|$ is proportional to the degree of baroclinic stability of a front, and is thus a natural measure of the position and intensity of a front.

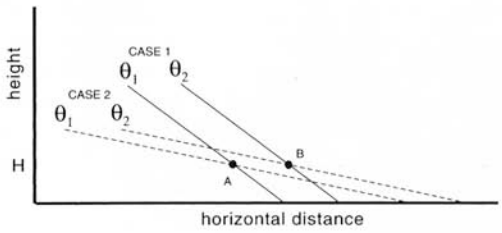

Fig. 1. Illustrating that a sloping inversion is considered as a relatively weak front when the frontal intensity is defined according to the slope of isentropes. 2 cases are shown: case 1 (solid lines) represents the typical configuration of the isentropes within an intense front; case 2 (dashed lines) represents the typical configuration of the isentropes if there is a sloping temperature inversion or stable layer. For the purpose of comparison, we specify the same horizontal gradient of the potential temperature in both cases. That is, the temperature difference between points A and B at a fixed height, H, is identical in both cases. Therefore, in terms of the Miller (1948) definition of frontal intensity, both fronts have equal intensity. However in terms of definition (1), the front in case 1 is more intense than in case 2.

There are 3 concerns with definition (1). First, the value of $|\boldsymbol{I}_F|$ goes to infinity when $\partial\theta/\partial z = 0$. However, except in the lowest few hundred metres of the atmosphere, $\partial\theta/\partial z$ is nearly always positive everywhere. This disadvantage becomes more acute when we use the equivalent potential temperature in eq. (1) instead of the potential temperature. A 2nd concern bears on the consequence of (1) that a nearly upright, broad frontal zone (i.e., characterized by weak static stability and a diffuse horizontal potential temperature gradient) is considered more intense than a nearly horizontal, narrow frontal zone (i.e., characterized by strong static stability and a concentrated horizontal potential temperature gradient). This consequence of (1) seems to contradict the implicit assumption that fronts should be narrow zones. We will necessarily not make this assumption here. A 3rd concern bears on the hypothetical idea that there may be cases where the isentropes steepen (i.e. static stability decreases) at the same that the magnitude of the horizontal potential temperature gradient decreases. This would be termed "frontolysis" according to the Miller–Petterssen definition, but not according the definition suggested in this paper.

2. Identifying fronts and their position

Let us apply these ideas to a summer frontal system approaching the western edge of Europe on 8 August 1992 (Fig. 2). Fig. 3 (left) shows the height of the 320 K isentropic surface at 0600 UTC

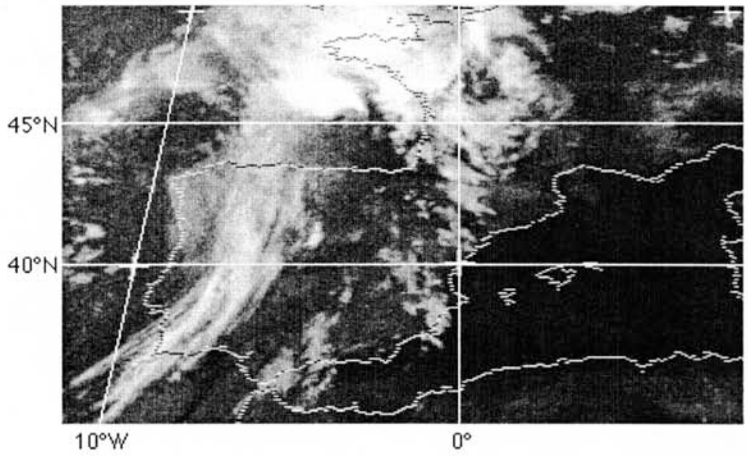

Fig. 2. Meteosat satellite image (infrared) of south-western Europe, corresponding to 8 August 1992, 05:30 UTC.

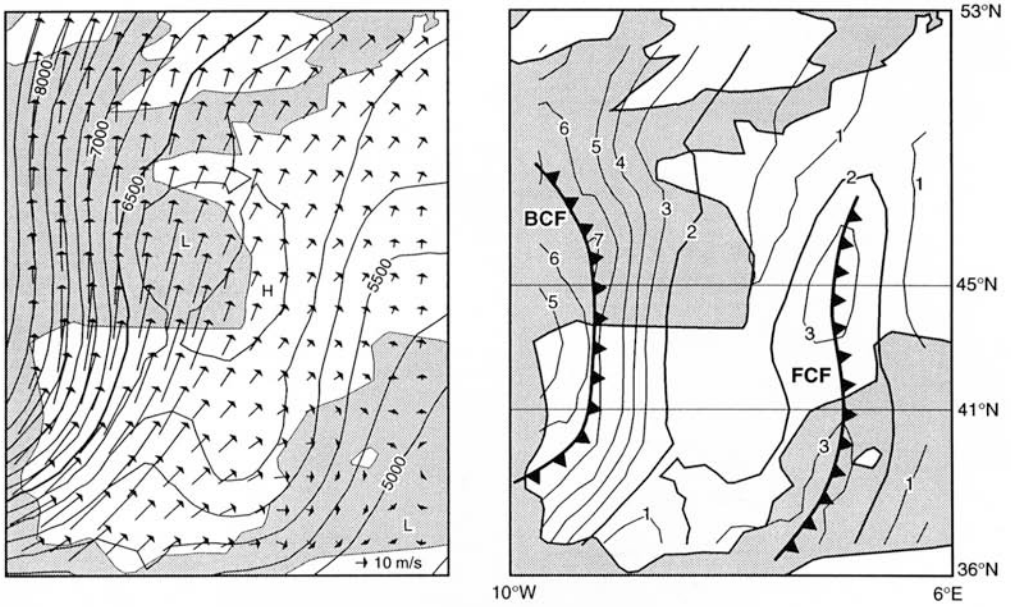

Fig. 3. Isopleths of the height of the 320 K isentropic surface labeled (m), wind vectors on this surface (left) and isopleths of the absolute value of the slope of the 320 K isentrope (right) (labeled in units of 10^{-3}), corresponding to 8 August 1992, 0600 UTC, derived from the ECMWF analysis on isobaric surfaces by linear interpolation. The FCF (forward cold front) and BCF (backward cold front) are discussed in the text.

on 8 August 1992 over southwestern Europe. In accordance with definition (1) of frontal intensity, *the position of the front on an isentropic surface can be defined as coinciding with the ridge in the contour plot of the slope of the isentropic surface.* In Fig. 3 (right) it can be seen that this definition yields two fronts on the 320 K surface, the *forward cold front* (FCF) and the *backward cold front* (BCF). Reasons for the use of this terminology will become apparent shortly. The BCF can be

recognized very clearly in the satellite image (Fig. 2) as the cloud band lying over western Iberia. The FCF is not that clearly recognized, although a connection with the band of scattered clouds over eastern Iberia (along the 0° meridian) is suspected.

A vertical/zonal cross section analysis of the potential temperature, the equivalent potential temperature and the circulation along the 45°N latitude band, approximately perpendicular to both fronts, is shown in Fig. 4, illustrating the disadvantage of using equivalent potential temperature in eq. (1). The 325 K isopleth of the equivalent potential temperature, for example, folds backwards, making the definition of its slope problematic. The isentropes, fortunately, do not exhibit this behaviour.

The fronts can be recognized in Fig. 4 by observing the enhanced slope of the isentropes. The FCF can be recognized easily leaning forward (towards the east) with increasing height. We will see in Section 4 that the forward tilt of the FCF is caused by the clearly discernible crossfrontal circulation associated with thermal wind adjustment of the front to the intensifying temperature contrast along the coast of western Europe. This may lead to the formation of severe thunderstorms (Van Delden, 1998). In fact, the FCF is a cold front of reduced static stability sloping toward the warm air, while the BCF is a cold front of increased static stability sloping toward the cold air. These types of fronts have been discussed also by, e.g., Bluestein (1993, p. 274), who remarked that the FCF does not fit the classical definition of frontal intensity.

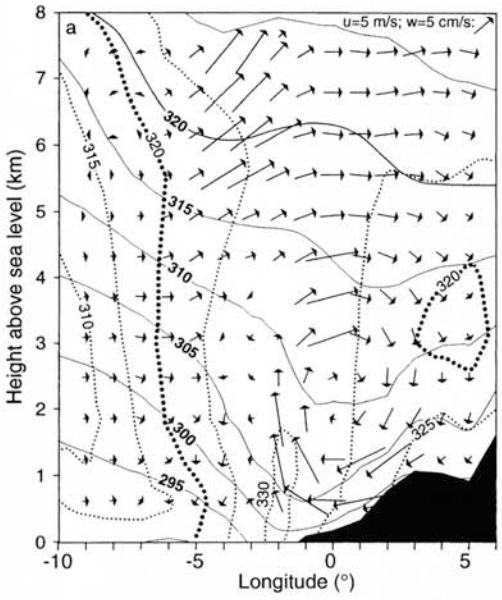

Fig. 4. Vertical/zonal section of the potential temperature (thin solid lines, labeled in K), equivalent potential temperature (dotted lines, labeled in K) and the component of the wind vector in the plane of the cross section at 45°N (Figs. 2, 3) corresponding to 8 August 1992, 0600 UTC, according to the ECMWF analysis. The orography of France, smoothed as in the ECMWF-model, is also shown.

A vertical/zonal cross section analysis of the frontal intensity along the 45°N latitude band, using the Miller–Petterssen definition of frontal intensity, $(\partial\theta/\partial x)_z$, is shown in Fig. 5 (upper panels) together with the analysis using $(\partial z/\partial x)_\theta$ as indicator of frontal intensity (lower panels). The fronts FCF and BCF are indicated explicitly in Fig. 5. Note, however, that other fronts may also be discerned, especially in the stratosphere and in the lower troposphere. For example, to the east of the FCF there is a warm front separating the warm air associated with the so-called "Spanish plume" (Van Delden, 1998) from the cooler air further to the east.

We see that the two definitions of frontal position and intensity give a similar description of the shape of the frontal system comprising the BCF and the FCF, but a somewhat different description of the relative intensity and intensification of these fronts. The definition in terms of the slope of isentropes (lower two panels) gives a FCF which intensifies between 0000 and 0600 UTC and exhibits an increasing forward tilt with increasing height. The Miller–Petterssen definition (upper two panels) hardly reveals the FCF. It also gives a weakening BCF, in contrast to the alternative definition. The Miller–Pettersen definition gives relatively stronger fronts in the stratosphere.

3. Analysing frontal intensification using the slope of isentropes

The rate of change of the x-component of the frontal intensity of a front moving with speed c_x in the x-direction and c_y in the y-direction is given

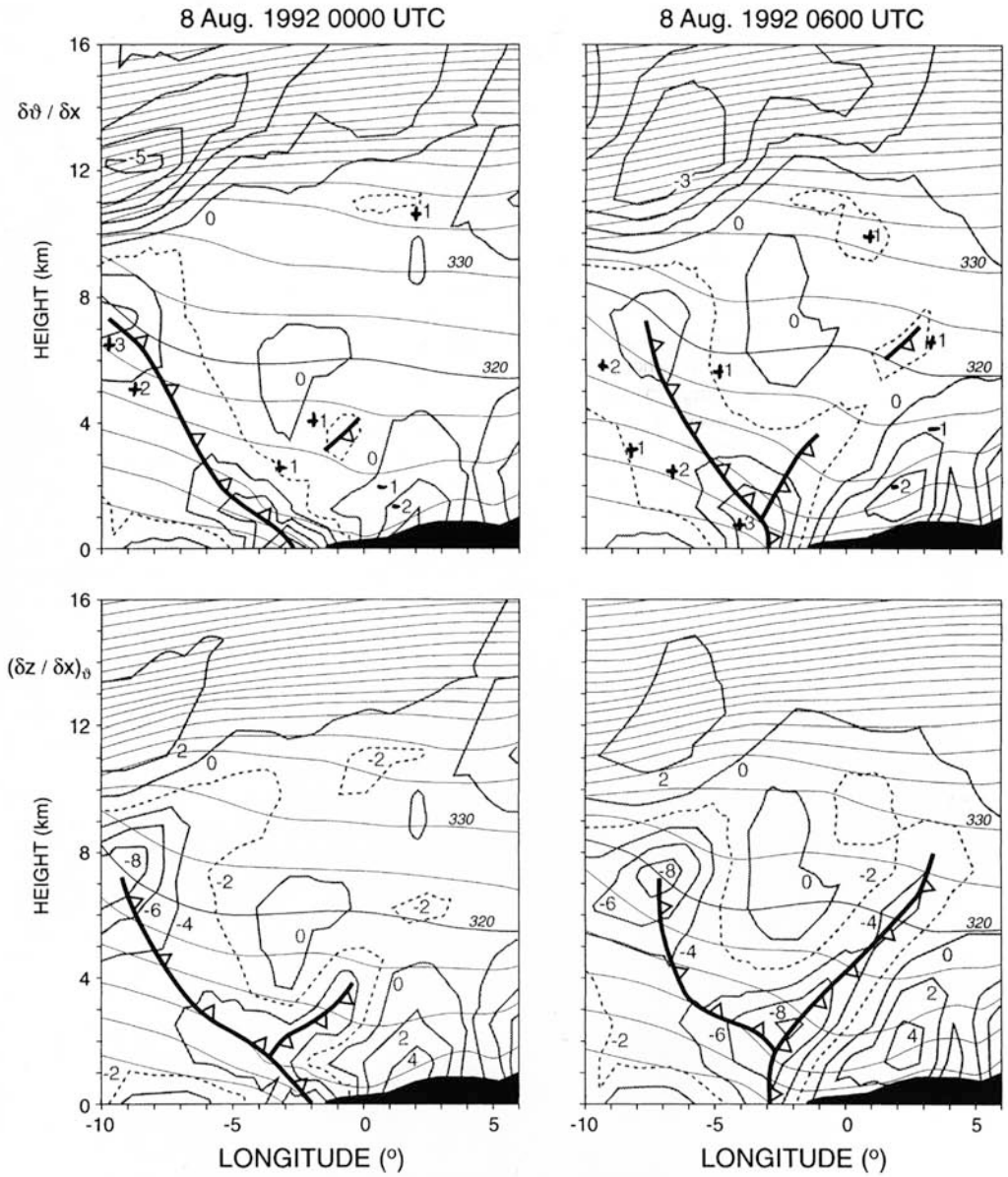

Fig. 5. The horizontal potential temperature gradient $(\partial\theta/\partial x)_z$ and of the slope of isentropes, $(\partial z/\partial x)_\theta$, as a function of height and longitude at 45°N (Fig. 3) corresponding to 8 August 1992, 0000 UTC (left) and 0600 UTC (right), according to the ECMWF analysis. Isopleths of potential temperature are indicated by thin solid lines (labeled in K), isopleths of $(\partial\theta/\partial x)_z$ in the upper panels are indicated by gray lines, labeled in units of 10^{-5} K m^{-1}, and isopleths of $(\partial z/\partial x)_\theta$ in the lower panels are indicated by gray lines, labeled in units of 10^{-3}. The fronts FCF and BCF are indicated explicitly. The orography of France, smoothed as in the ECMWF-model, is also shown.

by

$$\left[\frac{\partial I_{Fx}}{\partial t}\right]_{rel} = \frac{dI_{Fx}}{dt} - (u - c_x)\frac{\partial I_{Fx}}{\partial x} - (v - c_y)\frac{\partial I_{Fx}}{\partial y} - w\frac{\partial I_{Fx}}{\partial z}, \quad (2)$$

where the subscript "rel" indicates that the rate of change of I_{Fx} is evaluated in a reference frame moving with the same speed $\boldsymbol{c} = (c_x, c_y)$ of the front. We have assumed that the front does not propagate vertically. It must be remarked that it is very difficult, if not impossible, to determine $\boldsymbol{c}$ in practice. This becomes clear when observing (Fig. 5, lower panels) the change in the position of the frontal system between 0000 UTC and 0600 UTC on 8 August 1992. In the lowest km, the front actually moves westward ($c_x < 0$), while aloft it is approximately stationary or moves eastward ($c_x \geqslant 0$). The best choice for the value of c_x in this case would be zero.

The 1st term on the right-hand side of (2) can be evaluated as follows. The material change of I_{Fx} is given by:

$$\frac{d}{dt} I_{Fx} = \frac{\partial\theta}{\partial x}\left(\frac{\partial\theta}{\partial z}\right)^{-2}\frac{d}{dt}\left(\frac{\partial\theta}{\partial z}\right) - \left(\frac{\partial\theta}{\partial z}\right)^{-1}\frac{d}{dt}\left(\frac{\partial\theta}{\partial x}\right). \quad (3)$$

If $d\theta/dt$ (adiabatic conditions), then

$$\frac{d}{dt} I_{Fx} = I_{Fx}\left(-I_{Fx}\frac{\partial u}{\partial z} - I_{Fy}\frac{\partial v}{\partial z} + \frac{\partial w}{\partial z}\right) + \left(-I_{Fx}\frac{\partial u}{\partial x} - I_{Fy}\frac{\partial v}{\partial x} + \frac{\partial w}{\partial x}\right). \quad (4)$$

Therefore,

$$\left[\frac{\partial I_{Fx}}{\partial t}\right]_{rel} = I_{Fx}\left(-I_{Fx}\frac{\partial u}{\partial z} - I_{Fy}\frac{\partial v}{\partial z} + \frac{\partial w}{\partial z}\right) - I_{Fx}\frac{\partial u}{\partial x} - I_{Fy}\frac{\partial v}{\partial x} + \frac{\partial w}{\partial x} - (u - c_x)\frac{\partial I_{Fx}}{\partial x} - (v - c_y)\frac{\partial I_{Fx}}{\partial y} - w\frac{\partial I_{Fx}}{\partial z}. \quad (5)$$

In eq. (5) we see that changes in the intensity of a front are induced by the following mechanisms or effects: (a) $SH = -I_{Fx}^2(\partial u/\partial z)$, vertical shear of the horizontal component of the cross-frontal wind which tilts the isentropes to the vertical; (b) $ST = I_{Fx}(\partial w/\partial z)$, divergence of the vertical wind or "stretching"; (c) $CF = -I_{Fx}(\partial u/\partial x)$, confluence of the cross-frontal wind which increases the horizontal potential temperature gradient; (d) $TL = \partial w/\partial x$, cross-frontal horizontal shear of the vertical wind, which tilts the isentropes to the vertical; (e) $ADVX = -(u - c_x)(\partial I_{Fx}/\partial x)$, advection of frontal intensity in the zonal direction; (f) $ADVY = -(v - c_y)(\partial I_{Fx}/\partial y)$, advection of frontal intensity in the meridional direction; (g) $ADVZ = -w(\partial I_{Fx}/\partial z)$, vertical advection of frontal intensity; (h) $SHVX = -I_{Fy}(\partial v/\partial x)$, and (i) $SHVZ = -I_{Fx}I_{Fy}(\partial v/\partial z)$.

Strictly speaking, only the tilting-effect (d) is actually *frontogenetic*. The other mechanisms require the existence of a front and, thus, can only induce changes in the intensity of an existing front, or merely advect the front. However, most authors use the terms frontogenesis and frontolysis also to designate changes in the intensity of an existing front (Miller, 1948; Petterssen, 1956; Holton, 1992). We will adhere to this terminology here also.

Mechanisms SH, ST and SHVZ have no counterpart in the traditional approach to frontogenesis. This can be seen when we write down the equation for the intensity of frontogenesis defined by Miller (1948) as the rate of change of the horizontal gradient of θ following the motion. Restricting the analysis to adiabatic conditions, we may write:

$$\frac{d}{dt}\left(\frac{\partial\theta}{\partial x}\right) = -\frac{\partial\theta}{\partial x}\frac{\partial u}{\partial x} - \frac{\partial\theta}{\partial z}\frac{\partial w}{\partial x} - \frac{\partial\theta}{\partial y}\frac{\partial v}{\partial x}. \quad (6)$$

This equation should be compared with eq. (4). The first term on the right-hand side of eq. (6) is the counterpart of mechanism (c) or CF, the second term on the right-hand side of eq. (6) is the counterpart of mechanism (d) or TL and the third term on the right-hand side of eq. (6) is the counterpart of mechanism (h), or SHVX

Therefore, the alternative definition (2) of frontogenesis contains the frontogenetic mechanisms found in the traditional approach. Additional frontogenetic terms (i.e., SH, ST and SHVZ) appear, however, related to material changes in the static stability (the first term on the r.h.s. of eq. (3)).

4. Frontal intensification on 8 August 1992

Let us compute the frontogenetic terms in the case presented in Figs. 2–5. We will use the quantity,

$$\frac{I_{Fx}}{|I_{Fx}|}\left[\frac{\partial I_{Fx}}{\partial t}\right]_{rel},$$

which is positive when a front is intensifying and negative when a front is weakening. In Fig. 6a the average value of this quantity has been plotted as a function of height and longitude for the latitude-band 45°N–46°N, assuming $c_x = c_y = 0$.

There are two main centres or regions of frontal intensification, labeled "A" and "B", respectively in Fig. 6a. The frontal intensification in the region labeled "A" is responsible for the forward tilt of the FCF. The principal mechanisms contributing to this effect are TL and ADVX (Fig. 6b). The frontal intensification in the region labeled "B" can be attributed principally to the effect of confluence (CF), stretching (ST) and advection of the front in meridional (northerly) direction (ADVY). In the heart of the FCF (in the region labeled "C" in Fig. 6a), eq. (5) predicts a weakening of the front, principally due to TL. Due to the combined effect of these processes the front will tend to propagate towards the west at low levels and towards the east at upper levels, as is observed between 0000 and 0600 UTC (see the lower panels of Fig. 5), thus acquiring a stronger forward tilt.

Ogura and Portis (1982) investigated a similar case, with warm advection in advance of a cold front, a mid-tropospheric jet and a cross-frontal circulation with upward motion just above and slightly ahead of the position of the front at the earth's surface and downward motion on either side. They also found that the frontogenesis function is dominated by the tilting term, and that there is a tendency towards a forward tilt of the front with increasing height.

The rather exceptional forward tilt and intensity of the FCF observed along the western coast of France on 8 August 1992 is not observed everywhere along this front. In fact the FCF is hardly observed over northern Iberia (Fig. 7). Only weak remnants of a front leaning forward are observed at a latitude of 41–42°N and a height of about 6 km. By far the most intense frontal system in the troposphere at this latitude is the BCF.

The quantity,

$$\frac{I_{Fx}}{|I_{Fx}|}\left[\frac{\partial I_{Fx}}{\partial t}\right]_{rel}$$

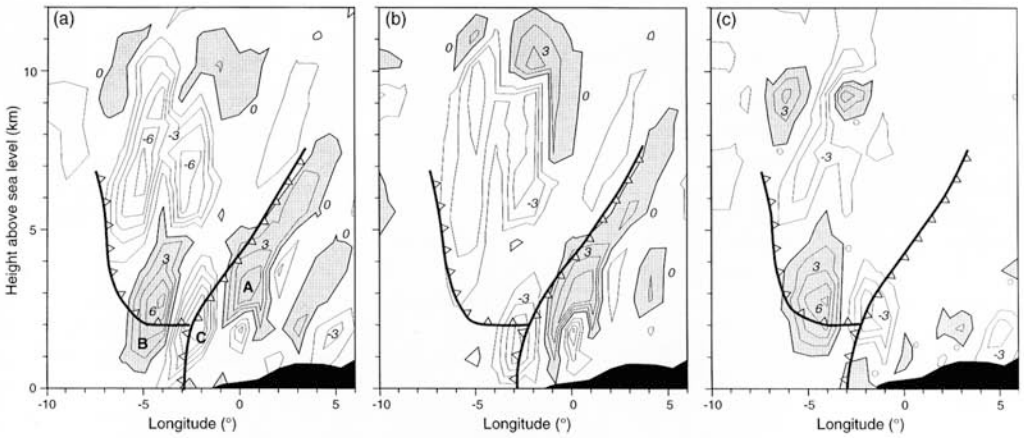

Fig. 6. Vertical/zonal section along the 45°–46° latitude band (Fig. 3) for 8 August 1992, 0600 UTC, according to the ECMWF analysis of (a) the quantity $(I_{Fx}/|I_{Fx}|)[\partial I_{Fx}/\partial t]_{rel}$, (b) the contribution of TL and ADVX to this quantity and (c) the contribution of all other adiabatic frontogenetic terms to this quantity. Isopleths of $(I_{Fx}/|I_{Fx}|)[\partial I_{Fx}/\partial t]_{rel}$ are labeled in units of $10^{-7}\,s^{-1}$. The letters A and B indicate separate areas of intense frontogenesis (see the text for further discussion). The letter C indicates an area of frontolysis (see text). The areas of frontogenesis ($(I_{Fx}/|I_{Fx}|)[\partial I_{Fx}/\partial t]_{rel} > 0$) are shaded. The frontal system (FCF + BCF) is indicated explicitly (see also Fig. 5).

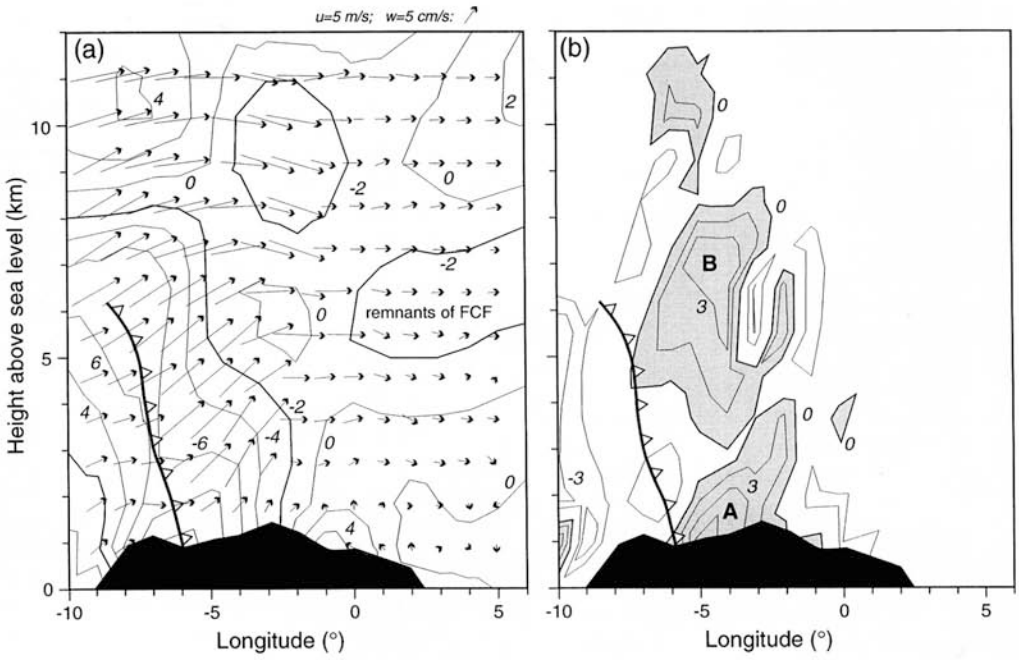

Fig. 7. Vertical/zonal section of (a) the mean slope of isentropes, $(\partial z/\partial x)_\theta$, and the average wind vector within this plane, and (b) the quantity $(I_{Fx}/|I_{Fx}|)[\partial I_{Fx}/\partial t]_{rel}$, along the 41°–42° latitude band (Fig. 3) for 8 August 1992, 0600 UTC, according to the ECMWF analysis. The orography of Iberia, smoothed as in the ECMWF-model, is also shown. In (a) isopleths of $(\partial z/\partial x)_\theta$ are indicated by solid lines, labeled in units of 10^{-3}. In (b) isopleths of $(I_{Fx}/|I_{Fx}|)[\partial I_{Fx}/\partial t]_{rel}$ are labeled in units of $10^{-7}\,s^{-1}$. The letters A and B indicate separate areas of intense frontogenesis (see the text for further discussion).

for this latitude-band is plotted in Fig. 7b, again assuming $c_x = c_y = 0$. We now observe two regions or centres of frontal intensification, labeled "A" and "B" respectively. In region A frontal intensification is principally due to CF and, to a lesser degree, SH and ST. In region B, TL appears to be the principle effect contributing to frontal intensification.

5. Conclusion

The principle reasons for suggesting the slope of isentropes as a diagnostic tool to represent frontal zones is its relation to the orientation in space of a material surface and its direct relevance to baroclinic instability, and therefore vertical motions. It is, however, not the intention of this paper to advocate the replacement of the traditional Miller–Petterssen definition of frontal intensity by a new definition. The traditional definition is a special case of the definition discussed in this paper. In fact, if we assume constant static stability, the definitions are identical (except for a constant factor).

The definition of frontal intensity in terms of the slope of isentropes brings out important features of frontal systems more clearly than the Miller–Petterssen definition. For instance, cold fronts leaning forward toward the warm air. These types of fronts, which do not fit the classical definition of fronts very well, are observed frequently in spring and summer over western Europe when warm air is advected northward at levels between 900 hPa and 700 hPa in advance of an approaching cold front.

A definition of frontal intensity should include a definition of the time rate of change of frontal

intensity, so that it can not only be used to locate fronts but also to identify whether a front will intensify or not, and through which physical effects. Compared to the fontogenesis equation based on the traditional definition, new frontogenetic terms, related to material changes in the static stability, appear in the frontogenesis equation based on the slopes of isentropes. In the example investigated here, these frontogenetic terms cannot be neglected, although they play only a secondary rôle. It appears that the tilting of isentropes due to cross-front horizontal shear of the vertical wind is by far the most important frontogenetic effect in the case investigated.

6. Acknowledgements

I would like to thank Seijo Kruizinga from KNMI (De Bilt) for helping me obtain the ECMWF analyses and the "AV-dienst" of the Institute for Earth Sciences for drawing the figures.

REFERENCES

Bluestein, C. B. 1993. *Synoptic-dynamic meteorology in midlatitudes*, vol. 2. Oxford University Press, New York, 594 pp.

Hewson, T. D. 1998. Objective fronts. *Meteorol. Appl.* **5**, 37–65.

Holton, J. R. 1992. *An introduction to dynamic meteorology*, 3rd edition. Academic Press, San Diego, 507 pp.

Huber-Pock, F. and Kress, Ch. 1989. An operational model of objective frontal analysis based on ECMWF products. *Meteorol. Atmos. Phys.* **40**, 170–180.

Miller, J. E. 1948. On the concept of frontogenesis. *J. Meteorol.* **5**, 169–171.

Ogura, Y. and Portis, D. 1982. Structure of the cold front observed in SESAME-AVE III and its comparison with the Hoskins–Bretherton model. *J. Atmos. Sci.* **39**, 2773–2792.

Petterssen, S. 1940. *Weather analysis and forecasting*, 1st edition. MacGraw-Hill, New York, 503 pp.

Petterssen, S. 1956. *Weather analysis and forecasting*, vol. 1, 2nd edition. McGraw-Hill, New York, 428 pp.

Renard, R. G. and Clarke, L. C. 1965. Experiments in numerical objective frontal analysis. *Mon. Wea. Rev.* **93**, 547–556.

Steinacker, R. A. 1992. Dynamical aspects of frontal analysis. *Meteorol. Atmos. Phys.* **48**, 93–103.

Van Delden, A. 1998. The synoptic setting of a thundery low and associated prefrontal squall line in Western Europe. *Meteorol. Atmos. Phys.* **65**, 113–131.